Journal of Applied Polymer Science

Polysulfone/Zinc Oxide Nanoparticle Mixed Matrix Membranes for CO_2/CH_4 Separation

Pourya Moradihamedani,[1] Nor Azowa Ibrahim,[1] Donya Ramimoghadam,[2] Wan Md Zin Wan Yunus,[3] Nor Azah Yusof[1]

[1]Department of Chemistry, Faculty of Science, Universiti Putra Malaysia, 43400 Serdang, Selangor, Malaysia

[2]Materials Synthesis and Characterization Laboratory (MSCL), Institute of Advanced Technology (ITMA), Universiti Putra Malaysia, 43400 UPM, Serdang, Selangor, Malaysia

[3]Department of Defence Science, Faculty of Defence Science and Technology, National Defence University of Malaysia, Sungai Besi Camp, 57000 Kuala Lumpur, Malaysia

Correspondence to: N. A. Ibrahim (E-mail: norazowa@science.upm.edu.my).

ABSTRACT: Preparation and characterization of novel polysulfone/zinc oxide (PSf/ZnO) mixed matrix membranes (MMMs) with different ZnO loadings for high selective CO_2/CH_4 separation were aimed in this study. Scanning electron microscopy photographs demonstrated that spongy and small tear like pores in plain PSf membrane (0 wt % of ZnO) replaced with large tear like pores close to surface layer by increasing ZnO content up to 0.1 and 1 wt %. In contrast, a dense and less free volume structure was obtained in membranes having 3 and 5 wt % of ZnO. Membrane porosity increased from 28.68 to 50.51% with increasing ZnO content from 0 to 1 wt %. Then, a reduction in porosity was observed for membranes containing 3 and 5 wt % of ZnO. Atomic force microscopy images presented variation in membrane surface roughness. Surface roughness decreased from 67.64 nm for plain PSf to 47.86 nm for membrane containing 1 wt % of ZnO. While, surface roughness increased and reached to 115.5 and 122.4 nm for MMMs having 3 and 5 wt % of ZnO. Gas separation properties of PSf/ZnO MMMs were examined and CO_2/CH_4 selectivity of MMMs containing 3 and 5 wt % of ZnO were 22.29 and 54.29, respectively, in 1 bar feed pressure. © 2013 Wiley Periodicals, Inc. J. Appl. Polym. Sci. 000: 000–000, 2013

KEYWORDS: membranes; separation techniques; morphology

Received 29 March 2013; accepted 8 July 2013; Published online 00 Month 2013

DOI: 10.1002/app.39745

INTRODUCTION

Application of membrane technology in gas separation process like hydrogen recovery from nitrogen, CO_2/CH_4 separation, and air separation is growing quickly. This is because of its low maintenance and space requirement, low power consumption, simple equipment, and mild procedure conditions.[1–4] Polymers are the most commonly used materials for the manufacture of membrane due to their desirable mechanical properties, flexibility to be developed in several modules, intrinsic properties of transport, and low cost.[5,6] However, the trade-off between permeability and selectivity is one of the significant challenges that severely restrict industrial usages of common polymeric membrane.[7,8] Therefore, employing of mixed matrix membranes (MMMs) has become very important in order to improve the gas separation and overcoming Robeson upper bound limitation. In general, MMMs be composed of organic polymer and inorganic fillers. Fillers are usually organized into two main categories namely porous and non-porous.[9] Current investigations have been motivated in improving the gas transport properties of polymeric membranes by a combination of nanoparticles.

There are many inorganic nanoparticles that have been used to prepare MMMs for gas separation such as, silica,[10–12] titanium dioxide,[7,13] magnesium oxide,[14] and Zeolite.[15,16] Silica as an usual non-porous filler has been widely used for fabrication of MMMs. Ahn et al.[17] employed non-porous fumed silica (FS) as fillers for the preparation of polysulfone (PSf)-silica MMMs. They found that the addition of this filler disrupted the polymer chain packing leading to a growth in free volume of the glassy polymer. Accordingly, the gas permeability increased considerably, but at the expense of selectivity. In another research, FS was used by Xing and Ho[18] as filler. They studied the performance of cross-linked polyvinyl alcohol/polysiloxane-FS including amine carriers for separation of CO_2 from H_2 at operating temperature and pressure conditions. According to their results, the CO_2 permeability and CO_2/H_2 selectivity reduced as the feed pressure increased due to the carrier saturation phenomenon.

Applied Polymer SCIENCE

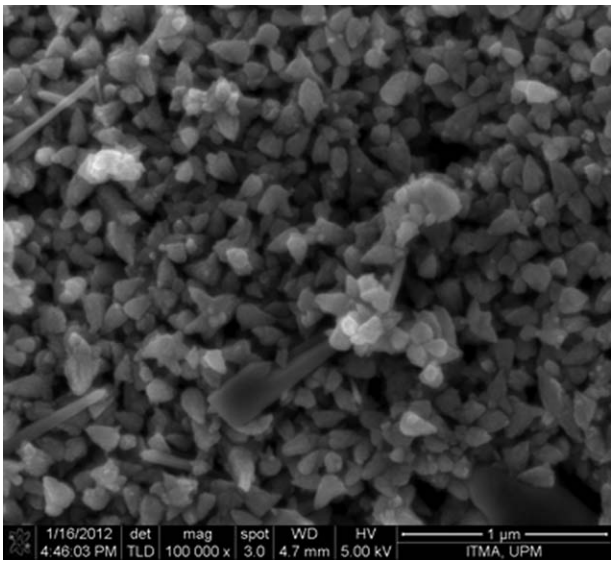

Figure 1. SEM photograph of prepared ZnO nanoparticles.

Also, the CO_2 permeability and CO_2/H_2 selectivity increased significantly as the gas relative humidities increased.

Moreover, zeolite as a common porous filler has been used in many MMMs. Valencia et al.[19] considered the preparation and characterization of ITQ-29/PSf MMMs for H_2/CH_4 separation. They examined the effects of zeolite composition and crystal size. Their result demonstrated that, the lower loading of zeolite in the membrane creates higher gas selectivity. The effect of zeolitic imidazolate frameworks on the gas transport performance of ZIF8-poly (1,4-phenylene ether ether sulfone) hybrid membranes was reported by Lopez et al.[20] According to their study, the permeability of hydrogen, nitrogen, oxygen, carbon dioxide, methane, ethane, and ethylene increased in a higher ZIF-8 loadings. Gas permeability increased in higher ZIF-8 concentrations without significant loss of selectivity. As a result, the higher the ZIF-8 loading, the better the membrane performance.

Although some studies surveyed the use of zinc oxide (ZnO) nanoparticles for fabrication of MMMs,[21–23] still the role of ZnO in MMMs for gas separation has not been reported. ZnO is more economical than other nanoparticle which being used for gas separation such as TiO_2 (~1/4 price according to the Chinese market quotes).[24] In addition, the supplementation of ZnO could improve mechanical properties of the polymer matrix.[25] Therefore, employing of ZnO in membranes is an innovative and promising technology which may be a key for the development of low cost and high performance membrane technology for gas separation. The novelty of this article is to clarify how usage of ZnO nanoparticles in PSf membrane could improve the CO_2/CH_4 separation properties of prepared membranes. This is the first time that the inclusion of ZnO nanoparticles into PSf membrane for CO_2/CH_4 separation is studied. Due to molecular sieving effect of ZnO, it is expected that higher concentration of ZnO improve selectivity of the membranes. Additionally, morphology, surface roughness, and thermal properties of prepared MMMs were studied in this work.

EXPERIMENTAL

Materials

PSf with the number average molecular weight (M_n) 22,000 was used as a base polymer due to its satisfactory gas permeance and selectivity purchased from Sigma-Aldrich, St. Louis, MO. PSf is an amorphous thermoplastic polymer with glass transition temperature of 190°C. This is a flame retardant polymer, possesses high mechanical, thermal, and oxidative stability and is soluble in common organic solvents.[26] Zinc acetate ($Zn(Ac)_2.2H_2O$), cetyltrimethylammonium bromide (CTAB, $C_{19}H_{42}BrN$), and sodium dodecyl sulfate (SDS, $C_{12}H_{25}SO_4Na$) from Sigma-Aldrich were used for preparation of ZnO nanoparticle. The organic solvents and non-solvent such as 1-methyl-2-pyrrolidone (NMP), tetrahydrofuran (THF), and isopropyl alcohol (IPA) were supplied from Merck, Frankfurter, Darmstadt, Germany. CO_2 and CH_4 gases were provided in 40 L cylinders with a purity of 99.99%. Distilled water was used as the second coagulation bath. The PSf resin was dried in an oven at 80°C for 24 h before the usage. Other chemicals were consumed as received.

Preparation of ZnO Nanoparticle

In a typical procedure, 1 g of zinc acetate ($Zn(Ac)_2\ 2H_2O$) and 2 g CTAB ($C_{19}H_{42}BrN$) were dissolved in 60 mL distilled water under constant stirring. The initial pH of the solution was recorded as 6.5 and then 5 mol L^{-1} NaOH solution was gradually introduced to the mentioned solution until pH reached to 13. Then, 1.44 g of SDS ($C_{12}H_{25}SO_4Na$) was added to the solution as the molar ratio of CATB : SDS equaled to 1 : 1. Finally, solution with white flocculent precipitate was transferred into a hydrothermal autoclave reactor with Teflon vessel of 50 mL (AT-HPV-50, Obromax, Maujpur, Delhi, India) and hydrothermal growth was carried out at 120°C for 18 h. After treatment, the autoclaves were allowed to cool down and the white precipitates were collected, centrifuged at 40,000 × *g* for 10 min and the supernatant was discarded. The obtained particles were washed three times with 50 mL ethanol and 50 mL distilled water separately in order to remove impurities and dried at 60°C for 24 h. Figure 1 shows the scanning electron microscopy (SEM) photograph of prepared ZnO nanoparticles.

Preparation of PSf/ZnO MMMs

In this study, flat sheet PSf/ZnO MMMs were prepared by wet/wet phase inversion technique. In wet/wet phase separation technique, membranes are prepared by contacting wet polymer film with two non-solvent baths in the series. The first coagulation bath is employed to obtain a concentrated layer of polymer at the interface. This step makes the ultra-thin surface layer. The purpose of second bath is the actual coagulation and formation of the final film. Casting solutions containing 22 wt % of PSf with different ZnO loadings (0.0, 0.1, 1.0, 3.0, and 5.0 wt %) were prepared using a mixture of NMP/THF as solvent with a ratio of 80/20 (V/V). Concentration of PSf in the casting solution was kept constant at 22 wt % maintaining concentration of solvent and ZnO in 78 wt %. The casting solution compositions of membranes are shown in Table I. The casting solution was stirred for at least 24 h. The polymer/nanoparticle mixture was then sonicated to ensure the ZnO dispersed homogeneously in

Table I. Different Casting Solution Compositions

PSf (wt %)	ZnO (wt %)	NMP (wt %)	THF (wt %)	Labeled as
22	0.0	62.40	15.60	PSf-0
22	0.1	62.32	15.58	PSf-0.1
22	1.0	61.60	15.40	PSf-1
22	3.0	60.00	15.00	PSf-3
22	5.0	58.40	14.60	PSf-5

the PSf solution then left standing for 1 day. Thirty minutes before casting, the mixture was sonicated again and then cast on a smooth glass plate by film casting knife to a thickness of 350 μm. The color of wet film changed from transparent to white immediately after immersion in the first coagulation bath containing IPA50%. Immersion time in the first coagulation bath was 90 s and after replacement of solvent by non-solvent, prepared membrane dipped in the distilled water for 24 h as a second coagulation bath. Finally, prepared membrane was dried at room temperature condition for 1 day.

Gas Permeation Experiments

Permeance of pure CO_2 and CH_4 gases were measured using gas permeation test in the pressure range of 1–7 bar at 25°C. Gas permeation mechanism of polymeric membrane is a solution-diffusion. Gases with a larger molecular diameter diffuse slower through the structure of prepared membrane.[2,27,28] Accordingly, since CH_4 molecular diameter is larger than CO_2,[28] prepared PSf/ZnO MMMs are able to separate these two gases by different selectivities. Stainless steel filter holder which was equipped with a back-pressure support screen with effective area of 13.8 cm^2 (Merck, Frankfurter, Darmstadt, Germany) was used. Glass soap bubble flow meter (Sigma-Aldrich, St. Louis, MO) was employed for measuring rate of permeate stream. To ensure accuracy in our experiments, the gas permeation test was repeated three times in the steady state. The gas permeability (P/L) was calculated using the eq. (1):

$$(P/L) = Q/(A \times \Delta P) \quad (1)$$

where P is permeability, L is membrane top layer thickness, Q is gas flow (at standard pressure and temperature), A is the effective membrane area in cm^2, and ΔP is the differential partial pressure across the membrane. The usual unit of permeance is GPU and 1 GPU is equal to 1×10^{-6} cm^3 (STP)/cm^2 s cm Hg. Equation (2) can be used to calculate CO_2/CH_4 selectivity. Where P_i and P_j are CO_2 and CH_4 permeance, respectively.

$$\alpha = P_i/P_j \quad (2)$$

Membrane Characterization

In order to investigate the morphology of membranes and evaluate ZnO nanoparticles distribution and agglomeration in polymer matrix, cross section photos were taken with SEM (LEO 1455 SEM, LEO & Leica factory, Cambridge, UK). Variations in surface roughness parameters of prepared MMMs were studied by atomic force microscopy (AFM) (Ambios Q-scope, Linthicum heights, MD) in tapping mode. The chemical interaction concerning PSf as base polymer and ZnO nanoparticle was evaluated by Fourier transform-infrared spectroscopy (Series100 PerkinElmer FT-IR 1650, Waltham, MA) in the wave number range of 280–4000 cm^{-1}. Energy dispersive X-ray (EDX) analysis was also conducted using an INCA instrument, (Oxford Instruments, Abingdon, Oxfordshire, UK) to confirm dispersion of the ZnO nanoparticles on the surface layer of prepared membrane. Thermal gravimetric analysis (TGA) (PerkinElmar TGA7, Waltham, MA) was conducted for identification of any variations in physical properties of membranes before and after cross-linking with a heating rate of 10°C min^{-1} from room temperature up to 700°C.

RESULTS AND DISCUSSION

Viscosity

The viscosity of polymer solution plays an important role in precipitation rate of wet film due to change of the phase demixing velocity of solvent and non-solvent. The viscosity of the prepared casting solutions with different ZnO contents were investigated using Brookfield digital viscometer (Model DV-II, Brookfield Eng. Middleboro, MA) at the constant temperature of 25°C. Variations in viscosity of casting solutions containing different amounts of ZnO are shown in Figure 2. As illustrated, casting solution viscosity increased gradually with ZnO concentration and reached to a maximum in 5 wt % of ZnO nanoparticle. The error bars are calculated from three separate viscosity measurements for different specimens. High specific area as well as high surface energy of ZnO nanoparticle considered a main reason to enhance the interaction among PSf macromolecules. Therefore, the viscosity of polymer solution increased obviously in higher ZnO concentrations. These results were in good agreement with the value in literature,[29] which reported that casting solution viscosity increased from 5.87×10^{-2} to 8.55×10^{-2} Pa s^{-1} in higher zirconia loading.

Membrane Morphology

SEM cross section views of prepared PSf/ZnO MMMs with different concentrations of ZnO in the casting solution in low and high magnifications are presented in Figure 3. As illustrated in Figure 3, all prepared membranes showed the asymmetric structure. Thickness of dried membranes was obtained by SEM photographs for PSf-0, PSf-1, PSf-3, and PSf-5 are 107.9, 78.18,

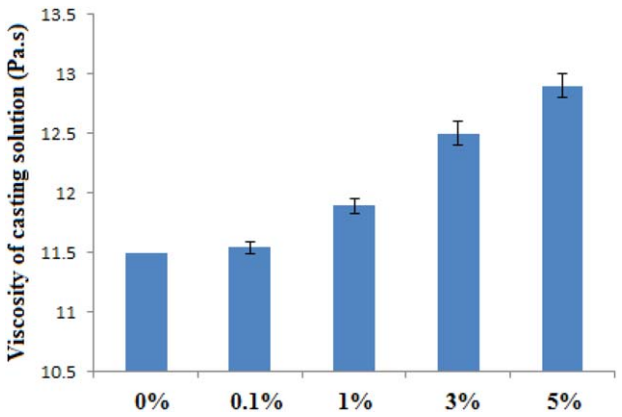

Figure 2. Viscosity of casting solutions in different ZnO loadings. [Color figure can be viewed in the online issue, which is available at wileyonlinelibrary.com.]

Applied Polymer SCIENCE

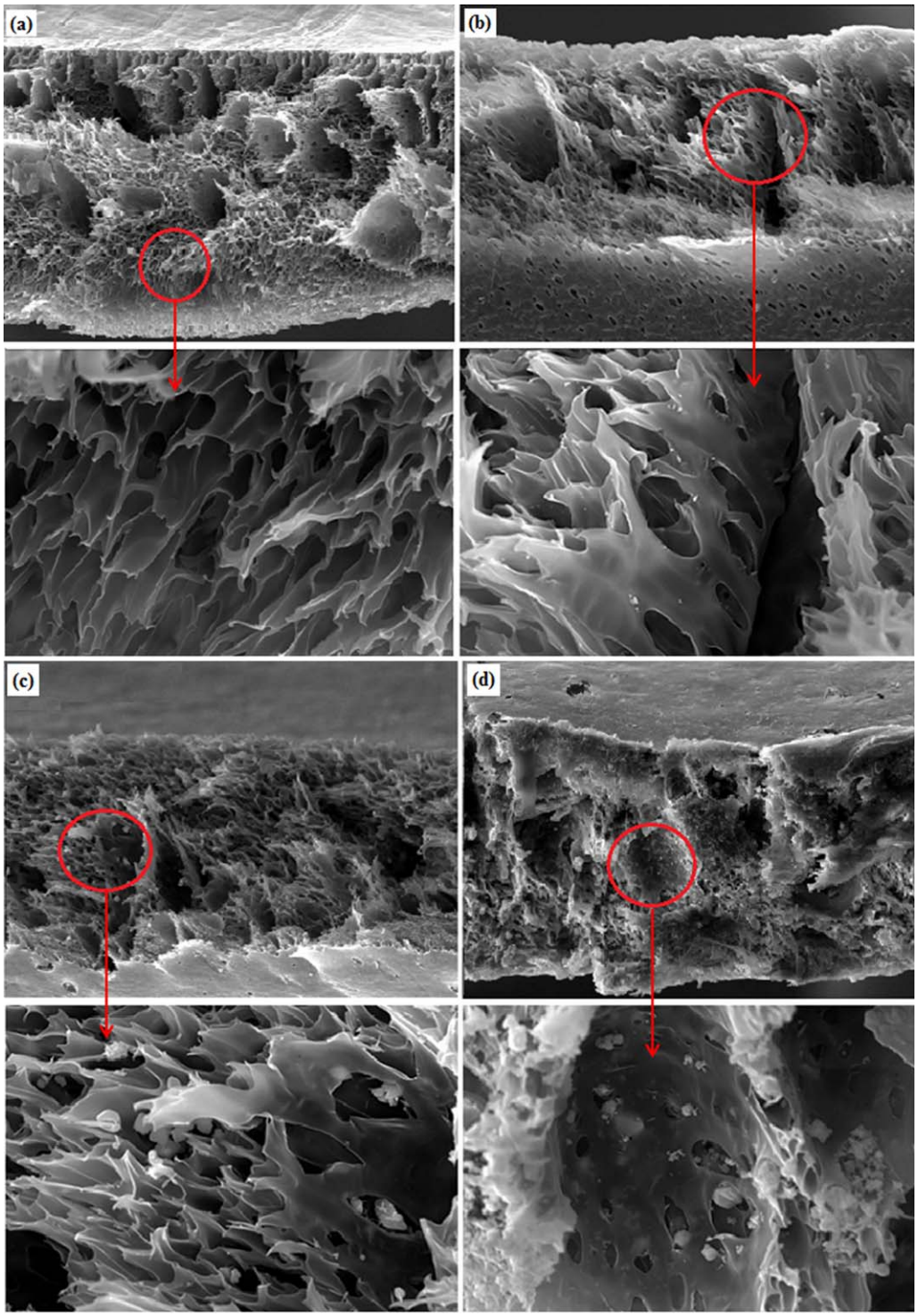

Figure 3. SEM photographs of PSf/ZnO MMMs with different ZnO concentrations: (a) 0 wt %, (b) 1 wt %, (c) 3 wt %, and (d) 5 wt %. [Color figure can be viewed in the online issue, which is available at wileyonlinelibrary.com.]

82.08, and 116.9 μm, respectively. Two different types of pore (spongy and tear like) are detectable from SEM photographs (Figure 3). Obviously, it could be viewed that the tear like pores which located at the upper layer of membranes became larger as the ZnO content going up from 0 to 1 wt % (Figure 3). SEM photos in higher magnification also proves that spongy structure in plain PSf membrane (0 wt % of ZnO) replaced by macro-void by addition of ZnO concentration until 1 wt %. Phase inversion kinetics have a considerable impact on the creation and development of macro-voids. Instantaneous liquid–liquid phase demixing is considered a main reason for the formation of macro-voids.[30] Since ZnO nanopaticles have

Table II. Variation in Surface Roughness Parameters with Different ZnO Loadings

Scanning area	Roughness		
20 × 20 μm^2	R_a (nm)	R_q (nm)	R_z (nm)
PSf-0	67.64	92.92	1305.00
PSf-0.1	56.47	80.31	919.20
PSf-1	47.86	72.51	837.30
PSf-3	115.50	174.50	1577.00
PSf-5	122.40	195.20	1614.00

higher affiliation with water than PSf, the velocity of water diffusion into the membrane structure increased in higher ZnO loadings (until 1 wt %) during phase inversion. The solvent transmission velocity from membrane to water could also be increased by addition of ZnO nanoparticle (until 1 wt %). As known, size of pore and membrane porosity improved with solvent diffusion speed.[31] In contrast, as shown in Figure 3 very less free volume structure containing spongy pores as a result of high interaction between ZnO and PSf[32] were obtained in MMMs containing 3 and 5 wt % of ZnO. Since increasing viscosity reduces the transmission velocity of solvent and nonsolvent, this results in delayed demixing which it may consider a void-suppressing function.[30] Thus, enhancement in polymer solution viscosity (Figure 2) causes macro-voids suppression.[33]

Surface Roughness Analysis

The morphology of surface layer in prepared MMMs in terms of the mean surface roughness (R_a) was analyzed by AFM in tapping mode (Figure 4). Samples with size of 20× 20 μm^2 surface area were scanned at 0.8 Hz. Roughness parameters were determined through the AFM analysis software (Nano scope Software Version). There exists mean roughness (R_a), root mean square of Z data (R_q), and mean difference in the height between the five highest peaks and the five lowest valleys (R_z). As presented in Table II, surface roughness parameters (R_a, R_q, and R_z) decreased clearly by adding ZnO from 0 to 0.1 and 1 wt %. Then, noticeable enhancement was observed in surface roughness parameters by increasing ZnO concentration from 1 to 3 and 5 wt %. The Z-value which is a distance between scanning tip and surface of sample has a key role in determination of roughness.[34] The higher peaks and deeper depressions in surface of samples, the more up and down movement of scanning tip which cause higher Z-value. The reduction in surface roughness parameters in low ZnO loading could be clarified by filling the pores of membrane as a result of entrapping ZnO nanoparticle in polymer film. Rahimpour et al.[35] reported same finding through entrapped TiO_2 nanoparticle in composite membrane. In contrast, accumulation of ZnO nanoparticle at the top layer of membrane may consider a main reason of surface roughness enhancement in MMMs containing 3 and 5 wt % of ZnO.

Membrane Porosity

The porosity of prepared PSf/ZnO MMMs containing different amounts of ZnO was calculated by eq. (3). Where, V_{void} is the void volume, V_{tot} is the total sample volume, V_{pol} is polymer volume, ρ is polymer density that is 1.24 g cm^{-3} for PSf, L is membrane thickness, A and m are effective area and weight of specimen, respectively.[36] Thickness of membrane was measured directly by SEM.

$$\varepsilon = V_{viod}/V_{tot} = (V_{tot} - V_{pol})/V_{tot} = [(L \times A) - (m/\rho)_{pol}]/(L \times A) \quad (3)$$

As illustrated in Figure 5, total membrane porosity increased from 28.68% to a maximum of 50.51% as ZnO concentration increased from 0 to 1 wt %. It could be explained by the

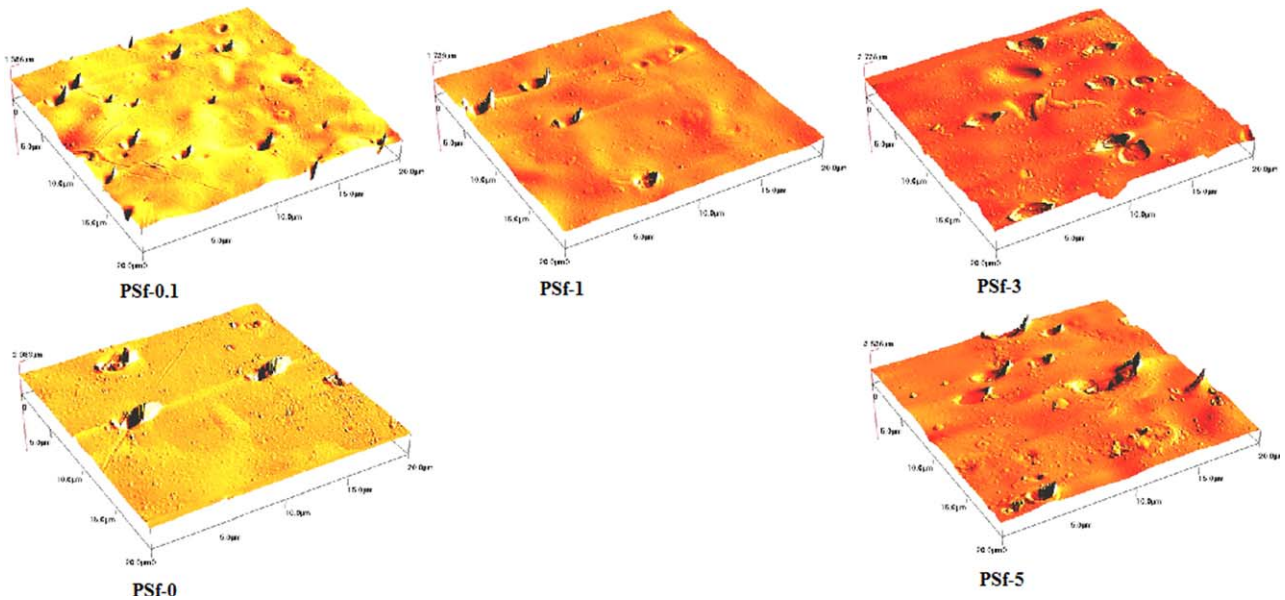

Figure 4. Three-dimensional AFM images of MMMs surface layer with different ZnO contents; (a) 0 wt %, (b) 0.1 wt %, (c) 1 wt %, (d) 3 wt %, and (e) 5 wt %. [Color figure can be viewed in the online issue, which is available at wileyonlinelibrary.com.]

Applied Polymer SCIENCE

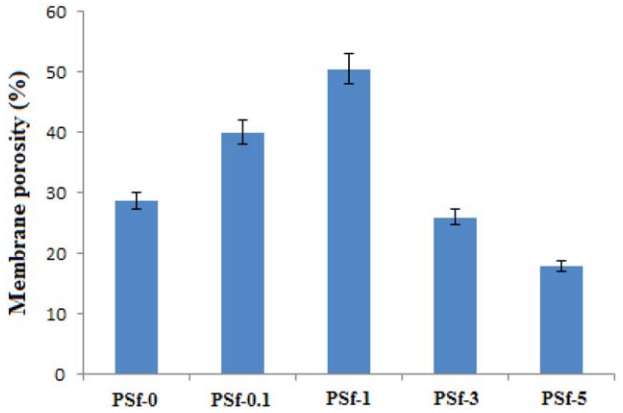

Figure 5. Variation in membrane porosity with different ZnO concentrations. [Color figure can be viewed in the online issue, which is available at wileyonlinelibrary.com.]

improvement of wet membrane hydrophilicity in higher ZnO content which cause instantaneous phase demixing between solvent (NMP/THF) and non-solvent (H_2O). While by increasing ZnO content from 1 to 3 and 5 wt %, membrane porosity decreased from 50.51 to 17.95%. The error bars are calculated from three separate porosity measurements for different specimens. Since viscosity of casting solution increased noticeably with ZnO content exceeded 1%, the velocity of solvent/non-solvent phase demixing declined remarkably. Then, delayed phase demixing between solvent and non-solvent has occurred that is the main reason for reduction of membrane porosity.[31]

FTIR and EDX Analysis

For better understanding of PSf and ZnO interaction at the molecular level, FTIR spectroscopy was used in the range of 280–4000 cm^{-1}. As illustrated in Figure 6 (PSf-0 spectra), two absorption peaks around 1270 and 1315 cm^{-1} indicating the symmetric O═S═O stretching vibration which was reported in FTIR spectra of the plain PSf[21] Symmetric and asymmetric

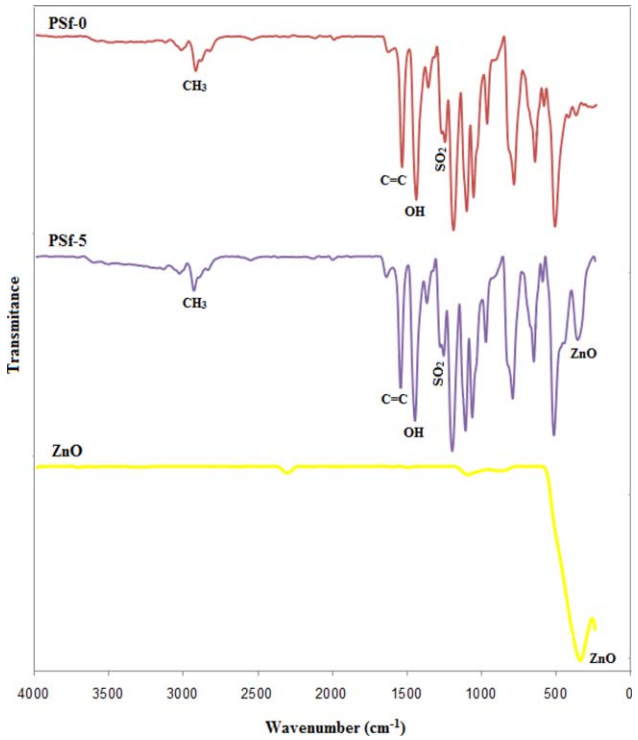

Figure 6. FTIR spectra of PSf-0, PSf-5, and pure ZnO. [Color figure can be viewed in the online issue, which is available at wileyonlinelibrary.com.]

deformation vibration of OH can be observed at 1355 and 1485 cm^{-1}, respectively. Also, high intensity peak at 1570 cm^{-1} was assigned to a C═C conjugation system of the benzene ring. A clear peak around 3000 cm^{-1} was noted for CH_3 stretching vibration.[37] As presented in Figure 7 (ZnO spectra), the high intensity peak near 400 cm^{-1} demonstrate the stretching mode of ZnO.[38] Hence, as presented in PSf-5 spectra (Figure 7), a single peak in the range of 400 cm^{-1} proves the presence of ZnO nanoparticle in prepared PSf-5 MMMs. Furthermore, to

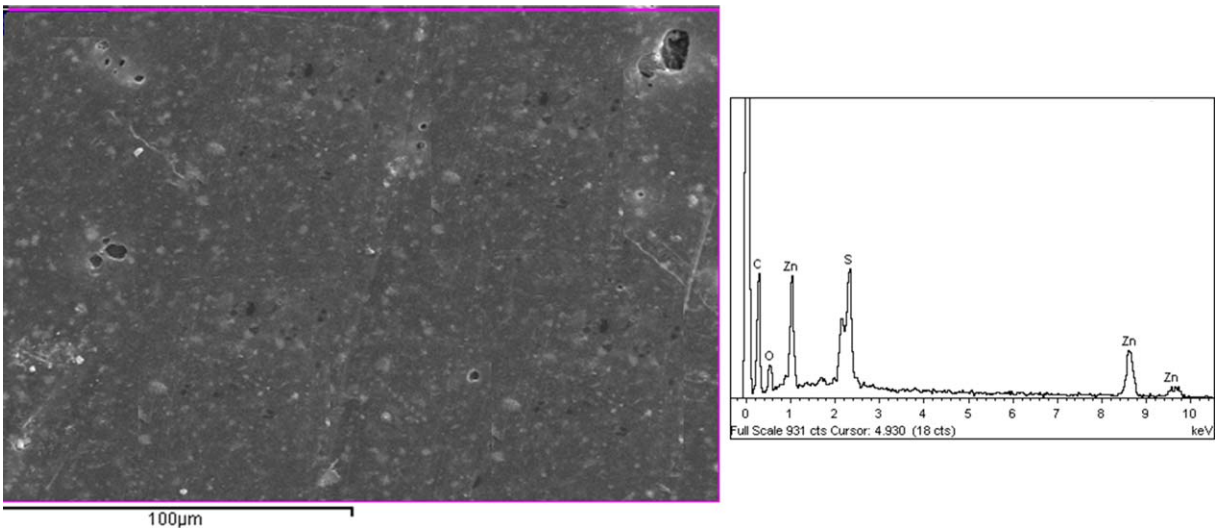

Figure 7. SEM photographs of PSf-5 membrane with respective EDX result.

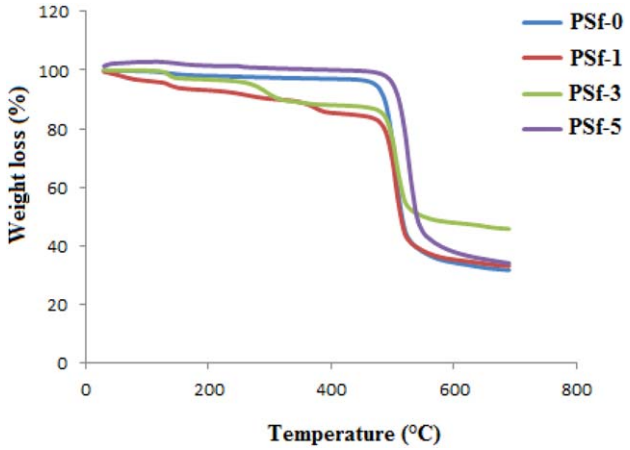

Figure 8. TGA curves of PSf/ZnO MMMs with different ZnO loadings. [Color figure can be viewed in the online issue, which is available at wileyonlinelibrary.com.]

confirm the distribution of ZnO nanoparticles on the top layer of prepared membrane, EDX analysis was used. EDX result in Figure 7 confirms existence and uniform distribution of nanoparticles in PSf-5 membrane.

TGA

TGA results of prepared membranes are shown in Figure 8. Due to solvent replacement by non-solvent in the coagulation bath, weight of specimens were approximately constant or decreased gradually in the temperature range of 25–500°C. A crucial weight loss has occurred in the temperature range of 500–550°C demonstrating decomposition of polymers. The amounts of weight loss for prepared PSf/ZnO MMMs decreased in the following order: PSf-0 (64.5%) > PSf-1 (61.29%) > PSf-3 (49.25%) > PSf-5 (39.05%). Accordingly, a reduction in the amount of weight loss was observed by increasing ZnO content in casting solution. This phenomenon shows that thermal stability of prepared MMMs improved in higher ZnO concentrations. This could be explained by the fact that ZnO has higher thermal stability compared to PSf.[22]

Gas Separation Evaluation

In this article, in order to examine the gas separation properties of prepared PSf/ZnO MMMs, CO_2 and CH_4 permeances of each membrane were measured separately in pressure range of 1–7 bar. As indicated in Figure 9, gas permeances of MMMs increased significantly with increasing ZnO content from 0 to 0.1 and 1 wt % (PSf-0, PSf-0.1, and PSf-1) in different feed pressures. The error bars are calculated from three separate permeability measurements for different specimens. Membrane porosity measurement (Figure 5) as well as cross section view of membranes (Figure 3), presented that membrane porosity increased and also spongy pores replaced with large tear like pores by increasing ZnO content from 0 to 1 wt % and then gas permeance of mentioned membranes increased. Since hydrophilicity of wet membranes improved in higher ZnO loadings, exchange velocity of solvent and non-solvent increased and instantaneous phase demixing between solvent and non-solvent has occurred which causes higher gas permeance through prepared membranes. In contrast, as demonstrated in Figure 9, CO_2 and CH_4 permeances declined with increasing ZnO concentration in the casting solution from 1 to 3 and 5 wt % (PSf-3 and PSf-5). Although higher ZnO content increases hydrophilicity of wet membranes, but the viscosity of polymeric matrix increased considerably in ZnO content exceeded 1 wt %. Accordingly, delayed phase inversion between solvent and non-solvent creates membranes with lower porosity (Figure 5) and less free volume structure (Figure 3) which it causes lower gas permeance for PSf-3 and PSf-5 MMMs.

CO_2/CH_4 selectivity of prepared PSf/ZnO MMMs displayed in Table III. As shown in this table, membrane selectivity dropped with increasing ZnO content from 0 to 0.1 and 1 wt % (PSf-0.1 and PSf-1) in different feed pressures and reached to a minimum in PSf-1 membrane. While, a distinct enhancement in gas selectivity was observed in membrane containing 3 and 5 wt % of ZnO (PSf-3 and PSf-5). As shown in Table III, the highest CO_2/CH_4 selectivity for PSf-3 and PSf-5 are 22.29 and 54.29, respectively, in 1 bar feed pressure. CO_2 permeances for these two membranes are around 10 and 8.5 GPU, respectively (Figure 9). These phenomena can be explained by variation in membrane porosity and also surface roughness in different ZnO loadings. As shown in Figure 5, membrane porosity reached to maximum for PSf-1 membrane which has lowest gas selectivity. However, PSf-5 membrane, which has the lowest amount of porosity, creates the highest gas selectivity among other prepared MMMs in this research. Furthermore, as illustrated in

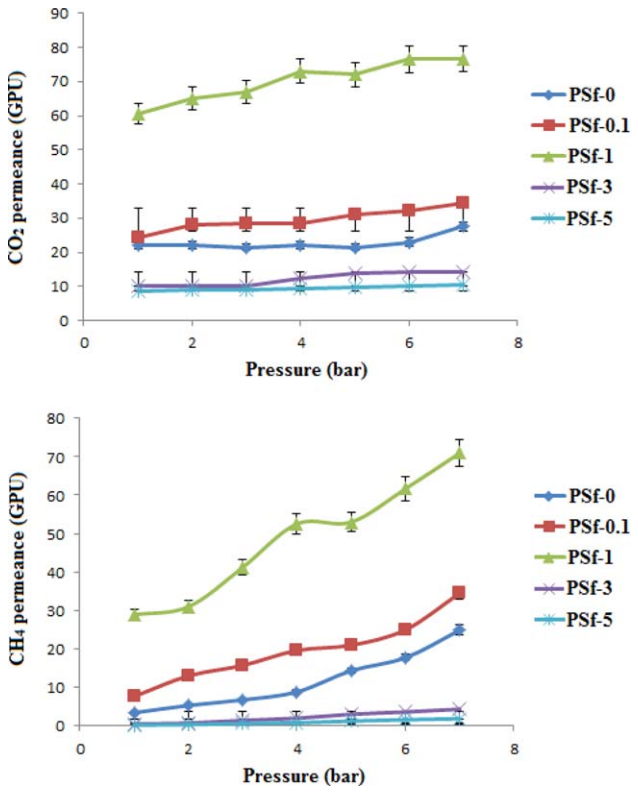

Figure 9. CO_2 and CH_4 permeances of PSf/ZnO MMMs with different ZnO contents. [Color figure can be viewed in the online issue, which is available at wileyonlinelibrary.com.]

Table III. CO_2/CH_4 Selectivity of Prepared MMMs in Different ZnO Concentrations

	CO_2/CH_4 selectivity (±0.10)						
Membrane ID/pressure	1	2	3	4	5	6	7
PSf-0	6.52	4.18	3.20	2.50	1.50	1.30	1.11
PSf-0.1	3.22	2.15	1.80	1.45	1.49	1.29	1.00
PSf-1	2.10	2.10	1.62	1.39	1.36	1.24	1.00
PSf-3	22.29	15.60	7.32	6.40	4.65	3.98	3.30
PSf-5	54.29	33.46	16.23	12.40	8.23	6.54	5.78

Figure 4 and also in Table II, surface roughness parameters of membranes decreased with increasing ZnO content up to 1 wt % and then an enhancement in surface roughness parameters was observed in MMMs containing 3 and 5 wt % of ZnO. In fact, higher surface roughness led to better separation properties of prepared membrane. Since gas permeation mechanism through polymeric membrane is a solution-diffusion and gases with larger molecular diameter defuse slower through membrane structure[2,27,28] and also because of larger molecular diameter of CH_4 in comparison with CO_2,[28] CO_2 permeability is higher than CH_4 permeability. Accordingly, a high selective CO_2/CH_4 separation has occurred by PSf-3 (22.29) and PSf-5 (54.29) MMMs.

CONCLUSIONS

The novel PSf/ZnO gas separation MMMs including different concentrations of ZnO nanoparticle were prepared. SEM characterization demonstrated that macrovoid structure converted to spongy and less free volume structure in higher ZnO concentrations (3 and 5 wt %). AFM images disclosed that surface roughness increased and reached to 115.5 and 122.40 nm^{-1} for PSf-3 and PSf-5, respectively. CO_2 and CH_4 permeances of membranes increased by increasing ZnO loadings and reached to maximum in 1 wt % of ZnO. While, a reduction in gas permeance was observed for MMMs with 3 and 5 wt %. Accordingly, CO_2 permeance reduced to around 10 and 8.5 GPU for PSf-3 and PSf-5 in 1 bar feed pressure. CO_2/CH_4 selectivity of prepared MMMs reduced in the following order: PSf-0 > PSf-0.1 > PSf-1. Interestingly, an improvement in gas selectivity of PSf/ZnO MMMs containing 3 and 5 wt % of ZnO was observed. The highest gas selectivity for PSf-3 and PSf-5 are 22.29 and 54.29, respectively, in 1 bar feed pressure. Less free volume structure and also higher membrane surface roughness are the main reasons of improving gas selectivity for PSf-3 and PSf-5 membranes.

REFERENCES

1. Dahe, G. J.; Teotia, R. S.; Bellare, J. R. *Chem. Eng. J.* **2012**, *197*, 398.
2. Dorosti, F.; Omidkhah, M. R.; Pedram, M. Z.; Moghadam, F. *Chem. Eng. J.* **2011**, *171*, 1469.
3. Sanaeepur, H.; Ebadi, A.; Moghadassi, A.; Kargari, A. *Sep. Purif. Technol.* **2011**, *80*, 499.
4. Ebadi, A.; Sanaeepur, H.; Kargari, A.; Moghadassi, A. *Sep. Purif. Technol.* **2012**, *82*, 102.
5. Clarizia, G.; Algieri, C.; Regina, A.; Drioli, E. *Microporous Mesoporous Mater.* **2008**, *115*, 67.
6. Arabi, A.; Kargari, A.; Bahrami, M.; Laki, S.; Ajami, H. J. *Ind. Eng. Chem.* **2013**, *19*, 677.
7. Moghadam, F.; Omidkhah, M. R.; Pedram, M. Z.; Dorosti, F. *Sep. Purif. Technol.* **2011**, *77*, 128.
8. Takht, M.; Kaghazchi, T.; Kargari, A. *Desalination* **2009**, *235*, 199.
9. Chung, T. S.; Jiang, L. Y.; Li, Y.; Kulprathipanja, S. *Prog. Polym. Sci.* **2007**, *32*, 483.
10. Wahab, M. F. A.; Ismail, A. F.; Shilton, S. J. *Sep. Purif. Technol.* **2012**, *86*, 41.
11. Zornoza, B.; Téllez, C.; Coronas, J. J. *Membr. Sci.* **2011**, *368*, 100.
12. Rafiq, S.; Man, Z.; Maulud, A.; Muhammad, N.; Maitra, S. *Sep. Purif. Technol.* **2012**, *90*, 162.
13. Liang, C.; Uchytil, P.; Petrychkovych, R.; Lai, Y.; Friess, K.; Sipek, M. *Sep. Purif. Technol.* **2012**, *92*, 57.
14. Saeid, S.; Li, Y.; Chung, T.; Liu, Y. J. *Membr. Sci.* **2007**, *302*, 207.
15. Gorgojo, P.; Uriel, S.; Te, C. *Microporous Mesoporous Mater.* **2008**, *115*, 85.
16. Bushell, A. F.; Attfield, M. P.; Mason, C. R.; Budd, P. M.; Yampolskii, Y.; Starannikova, L. J. *Membr. Sci.* **2013**, *427*, 48.
17. Ahn, J.; Chung, W.; Pinnau, I.; Guiver, M. D. J. *Membr. Sci.* **2008**, *314*, 123.
18. Xing, R.; Ho, W. S. W. *J. Membr. Sci.* **2011**, *367*, 91.
19. Valencia, S.; Corma, A.; Casado-coterillo, C.; Soto, J.; Te, C. *Chem. Eng. Sci.* **2012**, *73*, 116.
20. López-gonzález, M.; Luis, F.; Riande, E. J. *Membr. Sci.* **2011**, *383*, 206.
21. Balta, S.; Sotto, A.; Luis, P.; Benea, L.; Bruggen, B. V. D.; Kim, J. J. *Membr. Sci.* **2012**, *389*, 155.
22. Leo, C. P.; Lee, W. P. C.; Ahmad, A. L.; Mohammad, A. W. *Sep. Purif. Technol.* **2012**, *89*, 51.
23. Hong, J.; He, Y. *Desalination* **2012**, *302*, 71.
24. Liang, S.; Xiao, K.; Mo, Y.; Huang, X. J. *Membr. Sci.* **2012**, 394–395, *184*.
25. Tang, E.; Cheng, G.; Ma, X. *Powder Technol.* **2006**, *161*, 209.
26. Madaeni, S. S.; Moradi, P. J. *Appl. Polym. Sci.* **2011**, *121*, 2157.
27. Madaeni, S. S.; Enayati, E.; Vatanpour, V. *Polymer* **2011**, *122*, 827.
28. Scholes, C. A.; Kentish, S. E.; Stevens, G. W. *Langmuir* **2008**, *1*, 52.
29. Zheng, Y. M.; Zou, S. W.; Nanayakkara, K. G. N.; Matsuura, T.; Chen, J. P. J. *Membr. Sci.* **2011**, *374*, 1.
30. Soroko, I.; Livingston, A. J. *Membr. Sci.* **2009**, *343*, 189.

31. Moradihamedani, P.; Ibrahim, N. A.; Yunus, W. Z. W.; Yusof, N. A. J. *Appl. Polym. Sci.* **2013**, 1.
32. Zhang, Y.; Musselman, I. H.; Ferraris, J. P.; Balkus, K. J. J. *Membr. Sci.* **2008**, *313*, 170.
33. Yu, L. Y.; Xu, Z. L.; Shen, H. M.; Yang, H. J. *Membr. Sci.* **2009**, *337*, 257.
34. Taylor, P.; Shirazi, M. M. A.; Bastani, D.; Kargari, A.; Tabatabaei, M. *Desalin. Water Treat.* **2013**, 37.
35. Rahimpour, A.; Jahanshahi, M.; Rajaeian, B.; Rahimnejad, M. *Desalination* **2011**, *278*, 343.
36. Jansen, J.; Macchione, M.; Drioli, E. J. *Membr. Sci.* **2005**, *255*, 167.
37. Zhang, Y.; Shan, L.; Tu, Z.; Zhang, Y. *Sep. Purif. Technol.* **2008**, *63*, 207.
38. Zheng, J.; Ozisik, R.; Siegel, R. W. *Polymer* **2005**, *46*, 10873.